

Article

Removal of Cu(II) Ions from Aqueous Solutions by Ferrochrome Ash: Investigation of Mechanism and Kinetics

Erdoğan Uğurlu , Burak Birol *, Metin Gencten and Yahya Bayrak

Department of Metallurgical and Materials Engineering, Yildiz Technical University, 34210 Istanbul, Turkey

* Correspondence: bbirol@yildiz.edu.tr; Tel.: +90-212-3834661

Abstract: The release of Cu into water is an immediate concern that negatively affects environmental health. To eliminate this problem, the adsorption of Cu(II) on varying substances has been studied widely for two decades. The utilization of low-cost adsorbents obtained from industrial wastes hits two targets with one arrow. In the present study, ferrochrome ash (FCA) obtained from the baghouse filters of ferrochrome facilities was utilized to adsorb Cu(II) for the first time in the literature. To achieve this goal, initially the FCA was characterized by XRD, XRF, SEM, EDS, and BET analyses, and then washing and grinding pretreatment was conducted to eliminate the Cr dissolution and increase the surface area of the FCA. Adsorption experiments were conducted in 100–1000 mg/L Cu(II) solution on 0.4–8 g/L FCA for 0–300 min. As a result, it was concluded that a maximum adsorption capacity was obtained as 298.75 mg/g, which makes the FCA an applicable adsorbent for Cu(II) adsorption. Additionally, a pH range of 3–6 is favorable. The Cu(II) adsorption on FCA fits the pseudo-second order (PSO) kinetics and Freundlich isotherm models well. The Cu(II)-adsorbed FCA was investigated by SEM, EDS, and FT-IR analyses. According to the results, it can be deduced that the adsorption mechanism is chemisorption, which involves the valency forces between the metal and the adsorbent.

Keywords: water treatment; ferrochrome ash; Cu(II) adsorption; adsorption kinetics; adsorption isotherms



Citation: Uğurlu, E.; Birol, B.; Gencten, M.; Bayrak, Y. Removal of Cu(II) Ions from Aqueous Solutions by Ferrochrome Ash: Investigation of Mechanism and Kinetics. *Water* **2023**, *15*, 1063. <https://doi.org/10.3390/w15061063>

Academic Editor: Wei Wei

Received: 10 February 2023

Revised: 4 March 2023

Accepted: 8 March 2023

Published: 10 March 2023



Copyright: © 2023 by the authors. Licensee MDPI, Basel, Switzerland. This article is an open access article distributed under the terms and conditions of the Creative Commons Attribution (CC BY) license (<https://creativecommons.org/licenses/by/4.0/>).

1. Introduction

Heavy metal release to water resources from different production facilities is an important problem. The decrease in the rate of potable water worldwide rises substantially with the participation of heavy metal pollution [1]. From the Earth's origin, these heavy metals have been naturally occurring in the crust of the planet. Heavy metal use has dramatically increased, which has led to an impending rise in metallic contaminants throughout the terrestrial ecosystem and the freshwater habitats [2–4]. Contaminations originating from metals, such as lead, antimony, mercury, and copper, have an important place in heavy metal pollution considering the wide application area of the use of these metals [5]. Copper is one of the most important heavy metals, and is used in different application areas, such as metalworking processes, plastics, building constructions, electric and electronic products, etc. [6]. The contamination of copper in water can be caused from natural (forest fires, eruptions, and windblown dust) or man-made (mining, metal production, domestic, etc.) sources [4,7]. Therefore, the release of copper used in these processes into the environment through wastewater poses an important risk for the environment, ecosystem, and human health [8]. Since the copper concentration in the wastewater obtained from these processes is generally very high, it is necessary to reduce the copper concentrations by subjecting these waters to a process before they are released into the environment [6,9]. According to the United States Environmental Protection Agency (USEPA) and World Health Organization, the limit for the copper concentration in drinking water should not exceed 1.3 mg/L and 2.0 mg/L, respectively [10,11].

Various methods, such as adsorption, membrane filtration, cementation, and electrochemical techniques, can be used to reduce the copper content of wastewater [6]. In cementation, copper is reduced to a metallic state by using a reductant, such as iron and zinc ions. Although this method is easy and useful, sacrificial metal consumption is the main disadvantage of this method [6,12]. Membrane filtration allows for the removal of copper ions from the wastewater. However, this method cannot be used in turbid water. Indeed, clogging of the membrane pores and local bacterial formations have the potential to pose significant obstacles in the removal of copper [6,13,14].

There is still a need for further research to apply electrochemical methods at an industrial scale. Furthermore, the energy cost of the process describes a problem that must be overcome [6]. In this regard, the adsorption process, which describes the adsorption of ions in the solution to the solid phase surface as a result of physical or chemical interactions, comes with important advantages, such as low cost, simple design, high efficiency, reuse of adsorbent, and low energy consumption [6,15]. In the adsorption process for the removal of copper from wastewater, the adsorbent plays a key role on the efficiency of the removal [9]. Modified natural materials, environmental or agricultural wastes, biopolymers or hydrogels, and industrial by-products can be used to effectively remove copper. In the first category, modified natural materials, such as zeolite and its composites, have great performance for copper removal. Although modification of these materials increases the efficiency of the removal of copper, it increases the cost of the process [16]. Additionally, magnetic field utilization for metal adsorption is also a new process to increase the removal efficiency. In this process, the magnetic susceptibility and chemical properties of both the adsorbent and the adsorbate affect the removal process [17–20].

Modification and/or secondary processes of environmental or agricultural wastes also increase the cost of copper removal [21]. On this point, industrial by-products have great potential as efficient adsorbents for copper removal from wastewater. Wang et al. (2016) used quenched blast furnace slag for the removal of copper, zinc, and cadmium ions. Although they used quenched blast furnace slag, a secondary process in the preparation of the adsorbent took a long time, and it was also an energy-required process [22]. Yehia et al. (2008) used unburned carbon separated from blast furnace flue dust for the removal of copper ions from the solution [23]. Although the materials used had a relatively low cost, the removal efficiency of the copper was around 80% in optimal conditions [23]. Buema et al. (2021) used modified fly ash to improve the efficiency of the removal of the copper ions according to the unmodified fly ash [24,25]. Although they increased the efficiency of the removal of the copper ions from the solution, the added steps on the modification process to fly ash increased the economical and time costs of the process [24]. According to the literature, there is still a need to search for new materials obtained from industrial by-products to effectively remove copper from wastewater. On the other hand, various studies have investigated the removal of heavy metal ion removal from aqueous solutions by magnesium silicates. Liu et al. (2017) prepared a $\text{Fe}_3\text{O}_4@\text{MgSi}$ composite to remove copper ions and obtained a Cu(II) adsorption capacity of 2198 mg/g [26]. Huang et al. (2017) synthesized porous magnesium silicate nanoparticles with a surface area of $650.50 \text{ m}^2/\text{g}$, exhibiting a Cu(II) adsorption capacity of 52.30 mg/g [27]. Liu et al. (2013) removed Cu(II) with an adsorption capacity of 100 mg/g by using chrysotile ($\text{Mg}_3(\text{Si}_2\text{O}_5)(\text{OH})_4$) prepared from asbestos tailing [28]. Additionally, Choong et al. (2018) claim that increasing the magnesium silicate amount on the activated carbon increases the adsorption capacity of Cu(II) from 165 to 369 mg/g [29].

Ferrochrome ash (FCA), which is a waste collected at the baghouse filters of the ferrochrome production process, is generated at a rate of 0.02–0.03 tons per ton of ferrochrome production, and is mainly composed of magnesium silicate [30–32]. However, there is no industrial utilization of this waste and, therefore, an application area is required to prevent it from accumulating in nature and polluting the environment. Due to the high magnesium silicate content and fine particle size of the FCA, its utilization as an adsorbent will allow this waste to find a more value-added use. The present study involves the investigation of

the usability of FCA as a novel adsorbent. To achieve this goal, FCA was used as an adsorbent for copper. Initially, the properties of FCA and the effects of washing and grinding as a pre-treatment on the removal of copper from a Cu(II) aqueous solution were investigated. Here, SEM/EDS, XRD, and BET analyzes were conducted to characterize FCA, and atomic absorption spectroscopy (AAS) analysis was carried out to determine the element amount in the solution. Then, important parameters, such as pH, amount of adsorbent, and the concentration of copper that affects the performance of the adsorption were studied.

2. Materials and Methods

2.1. Materials

The FCA used in this study was obtained from the bag filter of the high carbon ferrochrome production furnace located in “Eti Krom A.Ş. Elazığ, Turkey”. XRF analysis of the FCA was carried out by a Panalytical Epsilon4 X-ray fluorescence spectrometer (Panalytical, Malvern, UK). According to the XRF results, the FCA contains 37.9% MgO, 28.8% SiO₂, 8.5% Al₂O₃, 6.1% Cr₂O₃, 6.0% K₂O, 4.4% ZnO, 2.8% Fe₂O₃, with the remainder made up of other minor elements. An X-ray diffractometer (XRD, Philips PW 3710, Philips, Amsterdam, The Netherlands) was used to characterize FCA utilizing CuK radiation over a range of 10–90° and a scanning speed of 1°/min. The Joint Committee on Powder Diffraction Standards (JCPDS) database was used to categorize the detected patterns. The peaks obtained from the XRD analysis of the FCA are given in Figure 1a.

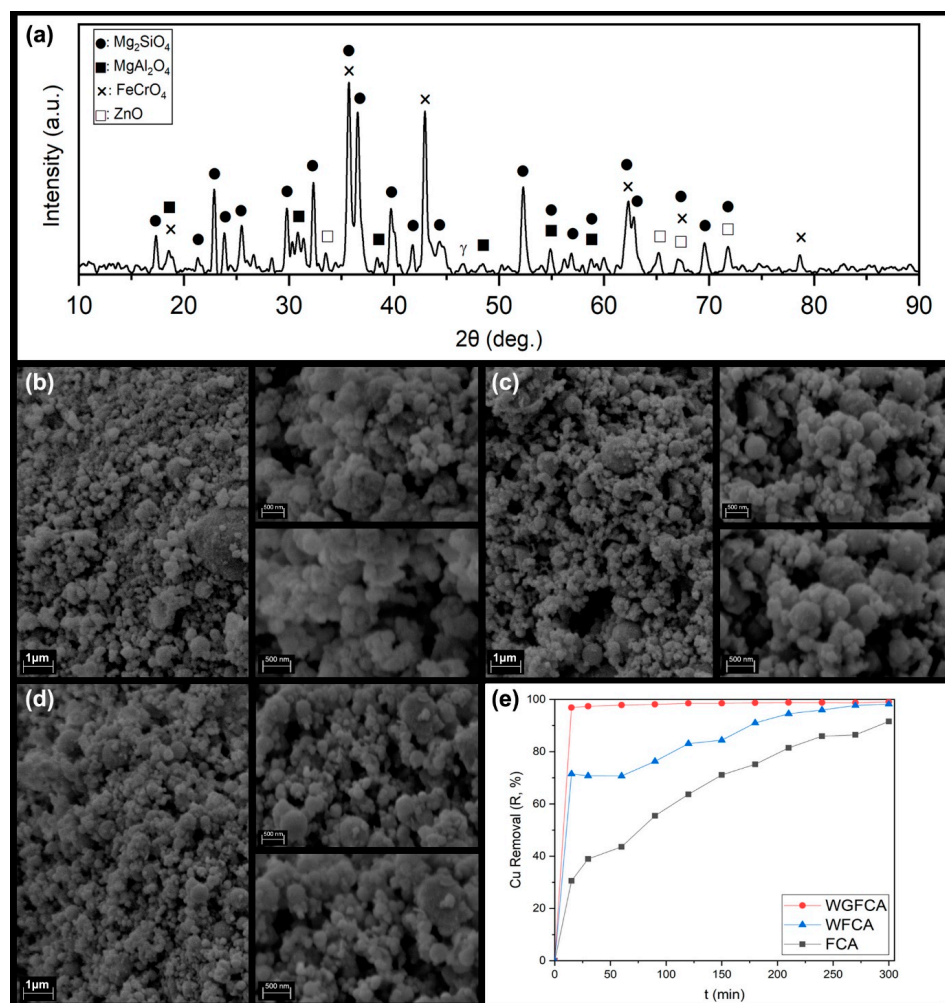


Figure 1. (a) XRD spectrum of the FCA; SEM images of (b) FCA, (c) WFCA, (d) WGFCa with $\times 20$ k, $\times 60$ k, and $\times 75$ k magnifications, and (e) R% values of the untreated and treated samples.

According to Figure 1a, the FCA is mainly composed of MgSiO_4 (ICSD: 00-004-0769) with relatively lesser amounts of MgAl_2O_4 (ICSD: 00-002-1084), FeCr_2O_4 (ICSD: 01-089-2618), and ZnO (ICSD: 01-079-0208). To be able to eliminate the Zn, Cr, and Fe contamination, 20 g of FCA was washed in 500 ml deionized water for 1 h and then filtered. This cycle was conducted three times, and the final solid residue was dried in an oven at 80 degrees for 1 h. Additionally, to increase the removal efficiency of the FCA, a grinding process for 5 min with a frequency of 10 Hz by a Retsch Mixer Mill MM 200 (Retsch, Haan, Germany) was applied to the washed FCA. Brunauer–Emmett–Teller (BET) analysis was conducted to the FCA, washed FCA (WFCA) and washed and ground (WGFCa) by a Quantachrome Quadrosorb SI BET device (Quantachrome, Boynton Beach, FL, USA) which uses cold bath N_2 gas (77.3 K). Data acquisition and reduction were performed using QuadraWin software (version 7.0). Morphological properties of the samples were investigated by a Zeiss EVO LS 10 SEM/EDS device (Zeiss, Jena, Germany).

The solutions to be used in the adsorption process were formed from copper sulfate stock solution, which was initially prepared from analytical grade $\text{CuSO}_4 \cdot 5\text{H}_2\text{O}$ and deionized water with a concentration of 1000 mg/L. Then, the solutions were diluted by distilled water to obtain the desired concentrations. Furthermore, for the pH experiments, the pH was adjusted by using diluted sulfuric acid (H_2SO_4).

2.2. Adsorption Experiments

The batch Cu(II) adsorption experiments were carried out in a beaker containing 250 mL of copper sulfate solution with varying concentrations (100–1000 mg/L), pH values (2–4.7), and WGFCa amounts (0.1–2 g) for contact periods of 1–300 min. A magnetic stirrer was used in all experiments with a stirring speed of 500 RPMs. After each experiment solid–liquid separation was made by filtering and both the initial and final solutions were analyzed by atomic absorption spectroscopy (AAS) (Perkin Elmer AAnalyst 400, Perkin Elmer, Waltham, MA, USA). AAS analysis was conducted by using copper standard solution obtained from Sigma Aldrich (Burlington, MA, USA) with a 1000 ppm concentration. The experiments were conducted three times, and the average values were calculated as the final concentration within a max error range of $\pm 0.5\%$. Copper ion removal ratio (R, %) and the adsorption capacity (q_t , mg/g) at time t were calculated according to the following Equations (1) and (2) [15], respectively:

$$\text{Cu Removal (R, \%)} = \frac{C_0 - C_t}{C_0} \times 100 \quad (1)$$

$$q_t = \frac{(C_0 - C_t) \times V}{m} \quad (2)$$

where C_0 (mg/L) represents the initial concentration of copper ions in the solution, C_t (mg/L) denotes the concentration of copper ions at time t, V (L) refers to the volume of solution, and m (g) is the mass of FCA.

Fourier transform infrared spectroscopy (FT-IR) analysis was conducted to the Cu(II)-adsorbed WGFCa using a Bruker VERTEX 70v device (Bruker, Billerica, MA, USA). The highest wavelength range was specified to be $450\text{--}4000\text{ cm}^{-1}$, with a resolution of 4 cm^{-1} , and a wavenumber tolerance of 0.01 cm^{-1} .

2.3. Isotherm and Kinetics Modelling of Adsorption Processes

The quantitative description of the adsorption process of Cu(II) ions on WGFCa adsorbent was investigated by using Langmuir and Freundlich models. Furthermore, pseudo-first order (PFO) and pseudo-second order (PSO) models were used for the kinetic investigation of the batch adsorption process. The linear equations of these models are given in Table 1 [15].

Table 1. Isotherm and kinetic models used for the experimental data.

Model	Equation
	Isotherm models
Langmuir	$\frac{1}{q_e} = \frac{1}{q_{\max}} + \frac{1}{q_{\max} \times K_L} \times \frac{1}{C_e}$ (3)
Freundlich	$\log q_e = \log K_F + \frac{1}{n} \times \log C_e$ (4)
	Kinetics models
Pseudo-first order (PFO)	$\log(q_e - q_t) = \log q_e - K_1 \times t$ (5)
Pseudo-second order (PSO)	$\frac{t}{q_t} = \frac{1}{K_2 \times q_e^2} + \frac{t}{q_e}$ (6)

Notes: Abbreviations are as follows: q_e , equilibrium adsorption capacity, mg/g; q_{\max} , maximum adsorption capacity, that is derived from the model, mg/g; K_L , Langmuir constant; C_e , equilibrium concentration, mg/L; K_F , Freundlich constant; n , heterogeneity factor; K_1 , PFO rate constant, 1/min; K_2 , PSO rate constant, g/mg.min.

The best-fitting models were chosen depending on the correlation R^2 values obtained from the linear fitting of the experimental data.

3. Results and Discussion

3.1. The Effect of Pretreatment on FCA

FCA, which is obtained from the bag filters of a high carbon ferrochrome arc furnace, contains an amount of Cr, Zn, and Fe, generally bound in a complex compound. However, the presence of these elements may come out with the problem of leaching into water [33]. Therefore, some preliminary experiments were made to investigate the dissolution of these elements. A total of 1 g of untreated FCA was added to 250 mL of deionized water and stirred for 300 min. Then, the suspension was filtered and analyzed by AAS. The results revealed that the dissolution of Cr, Zn, and Fe was 64.53, 0.21, and 0.10 mg/L, respectively. Although Zn and Fe dissolution amounts can be ignored, Cr had a very high dissolution ratio. Hence, this problem was eliminated by triple washing pretreatment, and the amount of these elements was observed to be less than 0.01 mg/L after washing.

Furthermore, to examine the effect of different pretreatments on removal efficiency, 4 g/L of untreated and treated fly ash samples were processed for 300 min in 100 mg/L of copper-containing solution and the results were analyzed by AAS. The effects of washing, grinding, and both washing and grinding on Cu removal, calculated by Equation (1), are given in Figure 1e. Moreover, the SEM images of the raw, washed, and ground FCA samples with magnifications of 20 k, 60 k and 75 k are given in Figure 1b–d, respectively.

According to Figure 1b, a wide range of particles less than 1 μm in size are observed throughout the structure of untreated FCA. When the formation of the particles is investigated in detail, the particles seem to be bound together to form bigger particles. This results in relatively lower surface areas that negatively affect the adsorption properties. On the other hand, after washing, the bonds between the particles of the WFCA seem to lower due to the removal of elements that dissolved inside water, as shown in Figure 1c. Furthermore, Figure 1d illustrates the SEM micrographs of the WFCA particles, and finer particle size distribution than the former two is recognized. From the BET analysis results the surface areas of FCA, WFCA, and WGFCa were obtained as 8.401, 8.455, and 10.577 m^2/g , respectively. The copper removal of the samples is shown in Figure 1e. Although a considerable change in the surface area was not observed, both washing and grinding increase the surface area as well as the copper removal ratios. Moreover, both these pretreatments play an important role on the kinetics of the adsorption process. FCA removed Cu from the solution within 300 min, where the adsorption process ends for WFCA at the 200th min and WGFCa at the 15th min. It was previously reported that increasing the surface area of the adsorbent increases the rate of adsorption due to the higher availability of adsorption sites on adsorbent surface [34,35]. Therefore, WGFCa samples were selected for all the adsorption experiments.

3.2. The Effect of pH

To determine the effect of pH on the Cu adsorption properties, initially, 0.25 g (1 g/L) of WGFCFA was used as an adsorbent in a 250 mL solution containing 100 mg/L Cu. The stirring period of 1–300 min was selected to obtain equilibrium between the adsorbent and the solution. pH measurements were made at determined periods, and the pH value of 4.7 ± 0.1 was determined. Because insoluble $\text{Cu}(\text{OH})_2$ precipitates at pH values over 5 [28,36,37], acidic solution pHs of 2, 3, 4, and 4.7 (without pH adjustment) were investigated by adjusting the pH using dilute sulfuric acid (H_2SO_4). Calculated Cu removal (R %) and q_t values by Equations (1) and (2), are given in Figures 2a and 2b, respectively.

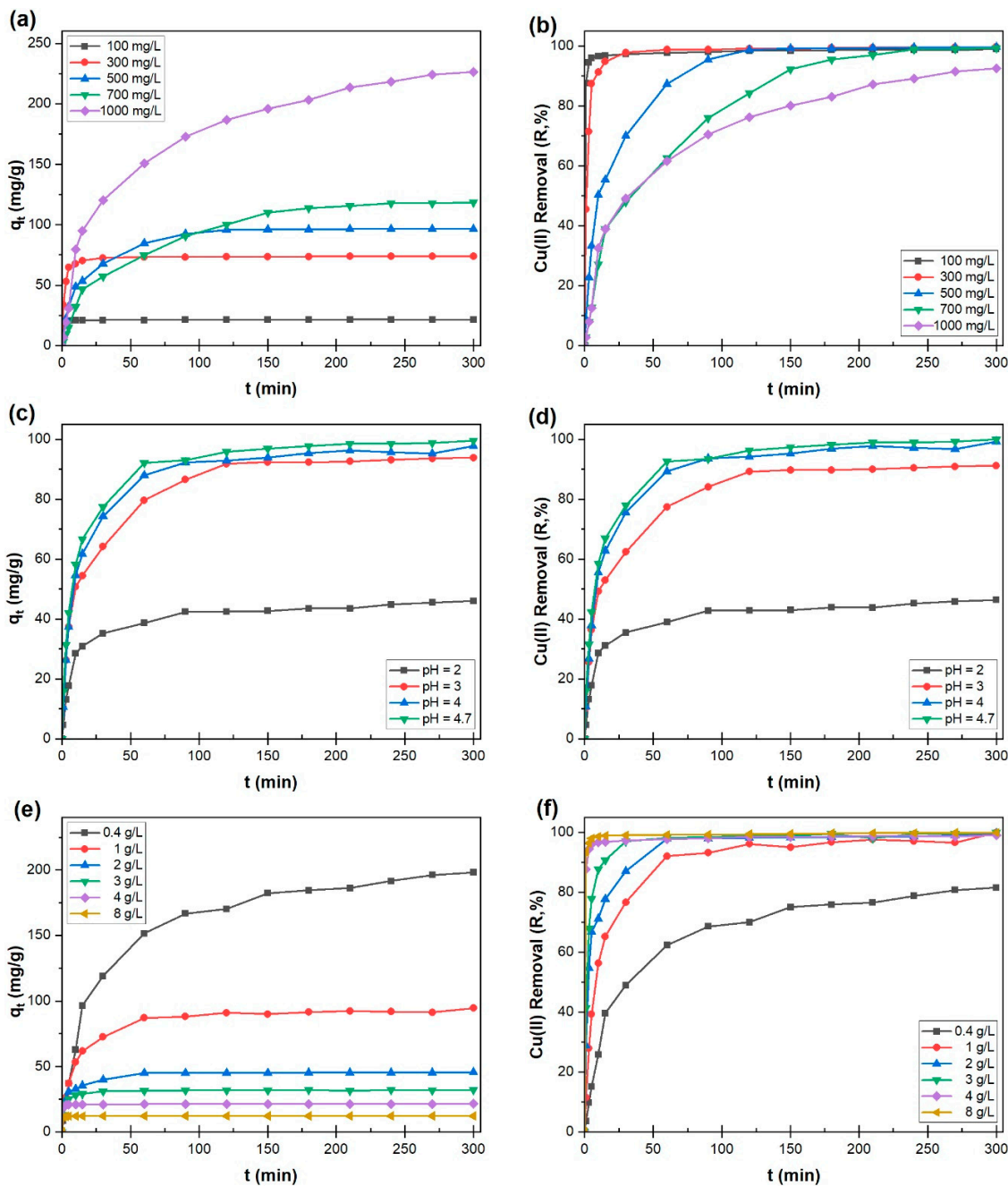


Figure 2. q_t values and copper removal (R%) to investigate the effect of (a,b) Cu concentration; (c,d) pH; (e,f) adsorbent amount.

pH plays an important role in the adsorption properties of Cu from aqueous solutions. As given in Figure 2c,d, the pH value of 2 has the lowest R and equilibrium adsorption capacity (q_e) values of 46.41% and 46.05 mg/g, respectively. Increasing the pH to 3 approximately doubles the Cu adsorption capacity. The pH values of 4 and 4.7 demonstrate almost similar R % values which are higher than 99%, with similar q_e values of 97.75 and 99.5 mg/g, respectively. Furthermore, increasing pH also increases the adsorption rate. For the experiment that was conducted at the pH value of 3, adsorption ended after 120 min, where at higher pH values 60–90 min was adequate for the adsorption reactions to reach completion. After that, a slight change was observed. These results are in good agreement with the literature, regardless of the organic or inorganic adsorbent type [37–41].

Abbar et al. (2017) defined the mechanism of the pH effect on the adsorption Cu(II) ions. At low pH ranges (0–2), excessive amounts of H^+ ions are present in the solution and the sorption sites of the adsorbent are saturated by H^+ ions. Due to the lack of empty sorption sites, Cu^{2+} ions would not be adequately adsorbed. When the pH range is between 2 and 4, because of the decreasing amount of H^+ ions, the availability of the sorption sites increases, and, therefore, Cu^{2+} can be adsorbed at these areas. Within the pH range of 4–6, the adsorption properties are slightly affected by the pH change. However at higher pH values, as a result of the increasing OH^- ions, $Cu(OH)_2$ precipitation begins to occur, and adsorption is affected negatively [42].

3.3. The Effect of Initial Metal Concentration

The initial metal concentrations of 100–1000 mg/L were studied to investigate the Cu adsorption properties of the WGFCFA. To achieve this goal, 1 g of WGFCFA was stirred in a 250 mL Cu solution with the concentrations of 100, 300, 500, 700, and 1000 mg/L for 1–300 min at a fixed pH of 4.7. The R and q_t values of the 4 g/L adsorbent-containing experiments are represented in Figure 2a,b, respectively. At low concentrations, the adsorbent immediately depleted the Cu(II) ions with high R values above 99% within 30 min. With the increasing initial metal concentration up to 700 mg/L, Cu also depletes ($R > 99\%$), but the completion time of the adsorption increases (500 mg/L in 120 min and 700 mg/L in 240 min). Additionally, q_e values obtained from the experiments increase proportionally with the initial concentrations from 21.4 to 118.3 mg/g. The experiment conducted for 1000 mg/L reaches a maximum R of 92.5% and a q_e of 226.5 mg/g in 300 min. An increment in the Cu(II) concentration stimulates the Cu(II) diffusion to the adsorbent surface, depending on the increasing propulsion of the concentration gradient which reduces the mass transfer resistance of Cu(II) between the solution and the adsorbent. [24,28,37–39]. From this result, it can be deduced that 4 g/L of adsorbent is not adequate to adsorb Cu(II) ions from a 1000 mg/L solution, because the sites that were available for adsorption were filled with Cu(II) ions. Figure 3 demonstrates the SEM and EDS analysis of the 4 g/L WGFCFA after 300 min of adsorption with 1000 mg/L initial metal concentration.

As given in Figure 3a,c, Cu accumulated on the surface area of the free sites located on the WGFCFA surface which was shown in Figure 1d. The EDS mapping of Cu (Figure 3b) reveals that a homogenous Cu distribution can be observed throughout the structure. Furthermore, when the structure is investigated in detail (Figure 3c), the copper is observed to have accumulated on the surface in an angular structure, and almost no free surface area is observed.

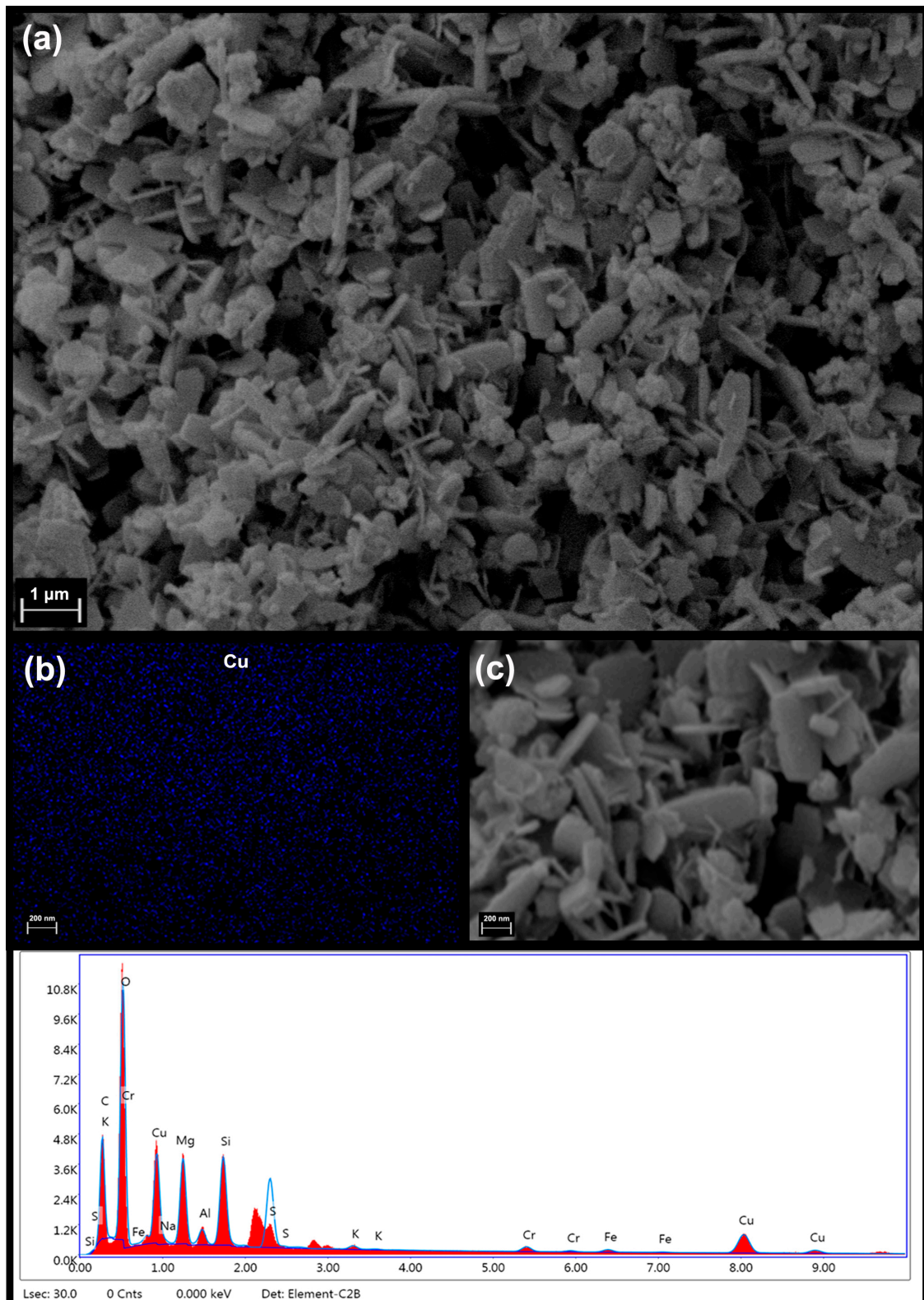


Figure 3. SEM micrograph (a) at 20k magnification, (b) EDS analysis, and (c) SEM micrograph at 75 k magnification of 4 g/L WGFCFA after 300 min of adsorption with 1000 mg/L initial metal concentration.

3.4. The Effect of Adsorbent Amount

The effect of the adsorbent amount was investigated by using 0.1–2 g (0.4–8 g/L) of adsorbent in the 100 mg/L Cu(II)-containing solution. Figure 2e,f display the R and q_t

change in the adsorbent amount experiments against time. Copper removal was efficiently made by the adsorbent amounts higher than 0.4 g/L with an R-value higher than 99% within 300 min. When the adsorbent amount was 4 and 8 g/L, the adsorption process was completed in a few minutes. However, lowering the adsorbent amount lowers the speed of the adsorption and inverse proportionally increases the time required for the adsorption to complete. Furthermore, the q_e values increased proportionally with the amounts between 1 and 8 g/L. According to Figure 2e,f, the R and q_e of the 0.4 g/L Cu(II)-containing experiments were, respectively, 81.5% and 198.1 mg/g.

3.5. Kinetic Investigation

A kinetic investigation was conducted by an adsorption process using 0.4 g/L adsorbent in 100–1000 mg/L of Cu(II)-containing solution for 0–240 min. The q_t and copper removal ratios are given in Figure 4a and 4b, respectively. In all the adsorption experiments, rapid removal was observed within 15 min. Then, the adsorption rate slowed down gradually until an equilibrium between the metal and the adsorbent was obtained. Although some fluctuations were observed after equilibrium was attained, a radical change in the q_t values was not encountered.

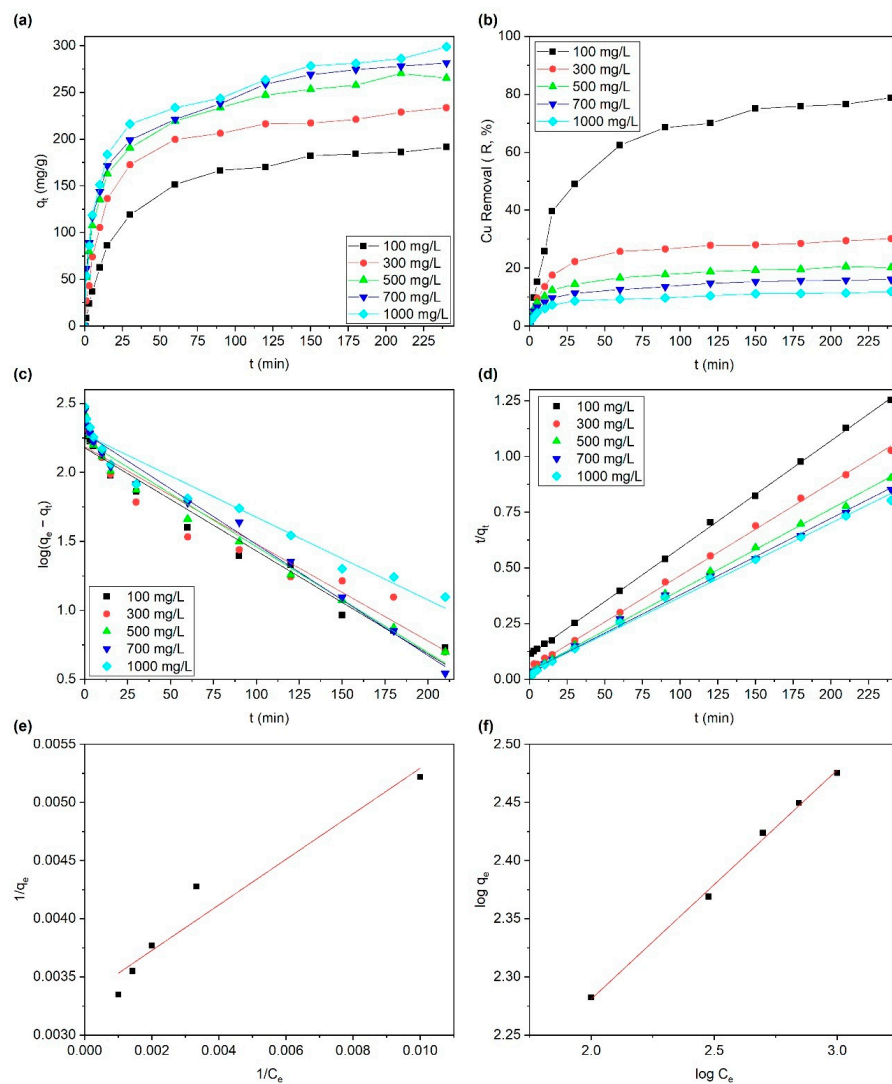


Figure 4. (a) q_t and (b) Cu removal of 0.4 g/L of WGFA in 100, 300, 500, 700, and 1000 mg/L Cu(II) concentration for 0–240 min; (c) PFO and (d) PSO kinetic model fittings; (e) Langmuir and (f) Freundlich isotherms.

Furthermore, pseudo-first order (Equation (5)) and pseudo-second order (Equation (6)) kinetic models were implemented for the kinetic experiments, and the data obtained are given in Table 2. The plots of both models for the metal concentration are also shown in Figure 4c,d. According to the results, both PFO and PSO models are able to determine the kinetics of the Cu(II) adsorption on WGFCFA with high coefficient of determination (R^2) values, which are over 0.93. On the other hand, the PSO model exhibits higher compatibility than the PFO model due to the R^2 values being higher than 0.995.

Table 2. Kinetic and isothermal parameters of the adsorption.

Kinetic Parameters							
Conc. (mg/L)	$q_{e, \text{exp}}$ (mg/g)	PFO			PSO		
		k_1 (1/min)	q_e (mg/g)	R^2	k_2 (g/mg.min)	q_e (mg/g)	R^2
100	191.56	0.000072	150.67	0.9727	0.00023	208.33	0.9996
300	233.81	0.000068	153.71	0.9308	0.00035	240.38	0.9989
500	265.35	0.000074	169.98	0.9721	0.00037	274.73	0.9978
700	281.6	0.000077	192.59	0.9807	0.00033	291.55	0.9964
1000	298.75	0.000057	188.17	0.9429	0.00152	300.3	0.9959
Isotherm Parameters							
Langmuir Model				Freundlich Model			
q_{max}	K_L	R_L	R^2	$1/n$	K_f	R^2	
299.4	0.017	0.37	0.9236	0.1969	77.14	0.9956	

According to the PFO model, the adsorption generally occurs at some specific areas, whereas, for the PSO, model adsorption is governed by chemisorption that involves the valency forces between the metal and adsorbent [24,43]. There are varying studies that investigate adsorbents containing magnesium silicates for the removal of heavy metal ions, where PSO is offered for Cu(II) adsorption [26–29,44,45]. Liu et al. (2007) used an adsorbent composed of iron oxide@magnesium silicate for Cu(II) adsorption and explained the adsorption mechanism as depending on the electrostatic attraction between the negatively charged silicate ions and the positively charged Cu(II) ions [26]. On the other hand, Huang et al. (2017) claimed that mechanically activated serpentine adsorbed Cu(II) at very high q_e values due to the Mg dissolution and copper precipitation in the form of wroewolfeite [44]. Furthermore, Petronias et al. (2020) confirmed the same adsorption mechanism [45]. Either way, Cu(II) adsorption is generally consistent with the PSO kinetic model.

3.6. Adsorption Isotherms

Adsorption values obtained from Cu(II) solutions with concentrations of 100, 300, 500, 700, and 1000 mg/L were fitted to Langmuir and Freundlich isotherm models to investigate the behavior between the Cu(II) and adsorbent. Figure 4e,f, respectively, illustrate the Langmuir and Freundlich isotherm fittings. Fitting and isotherm data given in Table 2 reveals that the Freundlich isotherm is more favorable than the Langmuir isotherm when relying on the R^2 values obtained. The value of R_L , which is the separation factor of Langmuir isotherm, defines the favorability of the model. The value of R_L can be irreversible ($R_L = 0$), favorable ($0 < R_L < 1$), linear ($R_L = 1$), or unfavorable ($R_L > 1$). The irreversibility of the system and the degree of favorability both contribute to a qualitative assessment of the interactions between adsorbent particles and heavy metal ions [42,46]. In the present work, the R_L value was determined as 0.37, where the Langmuir isotherm model seems favorable. The Langmuir isotherm is applicable for monolayer adsorption on homogenous surfaces, whereas the Freundlich isotherm is used for multilayer adsorption on heterogeneous surfaces [29,47]. K_F (mg/g) and $1/n$ values, which were obtained from the Freundlich isotherm, are the property constants that are related to the adsorption strength and the

heterogeneity of the adsorbent surface. When the $1/n$ constant is between $1 < n < 10$, it shows favorable adsorption [47], and the n value obtained in this study is 5.08. Therefore, a heterogeneous and multilayer adsorption mechanism can be mentioned for the Cu(II) adsorption on WGFCFA.

To determine the adsorption mechanism of Cu(II) ions on WGFCFA, FT-IR analyses were carried out. Figure 5 shows the FT-IR spectra of WGFCFA before and after Cu(II) adsorption. The peaks at around 900 and 1200 cm^{-1} were related with the Si-O-T bonds (T:Si or Al) in the chemical composition of FCA [48,49]. The bending mode of O-Mg-O can be seen at around 490 cm^{-1} [50]. The peaks of O-Si-O bonds were observed at 670 cm^{-1} [50]. Other peaks around 3360 cm^{-1} and 1600 cm^{-1} were attributed to -OH and H-O-H bonds [51]. As can be seen in Figure 5, the transmittance of peak, which was related with -OH, changed after the adsorption of Cu(II) ions. Indeed, the peak of hydroxyl was divided, caused by interactions of Cu(II) ions and hydroxyl groups. Positively charged Cu(II) ions were adsorbed on WGFCFA surface over oxygen atoms in hydroxyl groups consisting of partial negative charges [52,53]. Furthermore, Figure 6 illustrates the Cu(II) adsorption mechanism of WGFCFA.

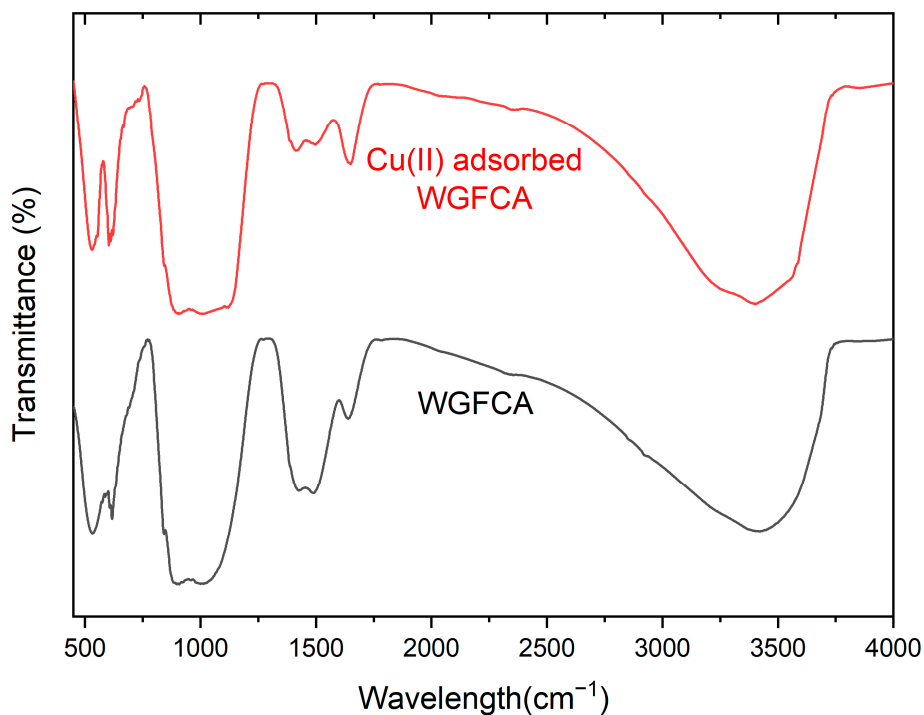


Figure 5. FT-IR spectra of WGFCFA before and after Cu adsorption.

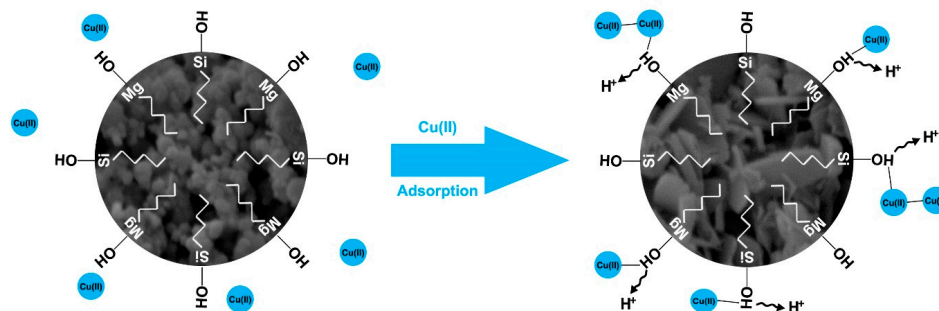


Figure 6. Illustration of the copper removal mechanism.

3.7. Comparison with the Literature

Numerous studies have investigated the adsorption mechanism of Cu(II) on various adsorbents; low-cost adsorbents obtained from waste attract special attention due to both economic and environmental concerns.

Table 3 represents the adsorption capacities of Cu(II) on varying adsorbents used in the literature and this work. It can be deduced that Cu(II) adsorption is generally compatible with the PSO kinetics model, where chemisorption is favorable. On the other hand, magnesium silicate-based adsorbents are commonly consistent with both the Langmuir and Freundlich isotherm models, while others recommend the Langmuir isotherm model only. Hence, a multilayer and heterogeneous adsorption mechanism can be specified where magnesium silicate is involved. When compared with the silicate-based or carbon-containing adsorbents, magnesium silicate-based adsorbents display higher Cu(II) adsorption capacities, as encountered in the present study.

Table 3. Cu(II) adsorption capacities of varying adsorbents.

Adsorbent	Recommended Kinetic Model	Recommended Isotherm Model	Adsorption Capacity (mg/g)	Reference
Silicate-based Adsorbents				
Maghnite	PSO	Langmuir	21.78	[39]
Water-quenched blast furnace slag	PSO	Langmuir	21.32	[22]
NaOH treated fly ash zeolite	PSO	-	27.90	[25]
Fly ash	PSO	Langmuir	69.93	[38]
Fly ash	-	Langmuir	8.54	[41]
Bentonite	Intra-particle diffusion	Langmuir	909.0	[54]
GMZ bentonite	PSO	Langmuir	6.23	[55]
Na-bentonite	PFO, PSO, Elovich's equation	Brunauer, Emmett, and Teller (BET)	-	[56]
Carbon-containing Adsorbents				
Peat moss	PSO	-	14.30	[57]
Rice bran	-	Langmuir	33.58	[36]
Sugar beet pulp	PFO, PSO	Langmuir	28.5	[37]
Palm shell activated carbon	-	Langmuir	1.581	[58]
Sawdust	PSO	Langmuir	263.2	[38]
Activated carbon	PSO	Langmuir	125.0	[38]
Unburned carbon from blast furnace flue dust	-	-	10.9	[23]
Lignite	PSO	Freundlich	21.0	[43]
Magnesium Silicate-based Adsorbents				
Chrysotile	PSO	Langmuir	86.85	[28]
Serpentine	-	-	50.00	[44]
Activated serpentine	-	-	539.0	[44]
Porous magnesium silicate with a flower-like structure	PSO	Langmuir	52.30	[27]
Magnetic magnesium silicate composite (Fe ₃ O ₄ @MgSi)	PSO	Langmuir, Freundlich	2198	[26]
Magnesium silicate impregnated palm shell waste	PSO	Freundlich	369.0	[29]
Washed and ground ferrochrome ash	PSO	Freundlich	298.75	This work

4. Conclusions

A novel adsorbent, mainly composed of magnesium silicate, namely ferrochrome ash, was utilized to adsorb Cu(II) in the present study, and the following conclusions were obtained:

1. A washing pretreatment was applied to the ferrochrome ash to remove hazardous Cr ions that would dissolve during the adsorption process. Furthermore, a grinding process was applied to be able to disaggregate the particles and increase the surface area of FCA.
2. pH levels lower than 3 influence the adsorption negatively due to the excessive H⁺ ions. On the other hand, when the pH value is higher than 6, precipitation of Cu(OH)₂ favors. Therefore, a range between 3 and 6 of pH value is favorable.
3. Up to 500 mg/L initial Cu concentration of the solution significantly increased the Cu(II) adsorption on 0.4 g/L WGFCFA and, at higher concentrations, a slight increase was observed.
4. Rapid adsorption was observed at the initial 15 min, and then the adsorption rate slowed down until an equilibrium was reached for all the samples. This behavior is coherent with the pseudo-second order of the kinetic model, which is explained with chemisorption.

Both the Langmuir and Freundlich isotherms are in accordance with the present study; however, the Freundlich isotherm fitting exhibited higher R² values. From this point of view, a heterogeneous and multilayer adsorption system is involved in the adsorption of Cu(II) on WGFCFA.

Author Contributions: Conceptualization, B.B. and M.G.; methodology, B.B. and M.G.; software, B.B.; validation, B.B. and M.G.; formal analysis, Y.B.; investigation, E.U.; resources, B.B.; data curation, Erdoğan Uğurlu, Y.B. and M.G.; writing—original draft preparation, E.U., B.B. and M.G.; writing—review and editing, B.B. and M.G.; visualization, B.B.; supervision, B.B. and M.G.; project administration, B.B. and M.G.; funding acquisition, B.B. and M.G. All authors have read and agreed to the published version of the manuscript.

Funding: This work has been supported by Yildiz Technical University Scientific Research Projects Coordination Unit under project number “FBA-2022-4987”.

Data Availability Statement: The datasets generated during and/or analyzed during the current study are available from the corresponding author on reasonable request.

Acknowledgments: The authors would like to express their gratitude towards Eti Krom A.Ş. Elazığ, Turkey, for supplying the ferrochrome ash used in the present work.

Conflicts of Interest: The authors declare no conflict of interest. The funders had no role in the design of the study; in the collection, analyses, or interpretation of data; in the writing of the manuscript; or in the decision to publish the results.

References

1. Chowdhury, S.; Mazumder, M.A.J.; Al-Attas, O.; Husain, T. Heavy Metals in Drinking Water: Occurrences, Implications, and Future Needs in Developing Countries. *Sci. Total Environ.* **2016**, *569–570*, 476–488. [\[CrossRef\]](#)
2. Briffa, J.; Sinagra, E.; Blundell, R. Heavy Metal Pollution in the Environment and Their Toxicological Effects on Humans. *Heliyon* **2020**, *6*, e04691. [\[CrossRef\]](#) [\[PubMed\]](#)
3. Szatyłowicz, E.; Krasowska, M. Assessment of Heavy Metals Leaching from Fly Ashes as an Indicator of Their Agricultural Use. *Desalin. Water Treat.* **2020**, *199*, 288–296. [\[CrossRef\]](#)
4. Łapiński, D.; Wiater, J.; Szatyłowicz, E. The Content of Heavy Metals in Waste as an Indicator Determining the Possibilities of Their Agricultural Use. *J. Ecol. Eng.* **2019**, *20*, 225–230. [\[CrossRef\]](#)
5. Vardhan, K.H.; Kumar, P.S.; Panda, R.C. A Review on Heavy Metal Pollution, Toxicity and Remedial Measures: Current Trends and Future Perspectives. *J. Mol. Liq.* **2019**, *290*, 111197. [\[CrossRef\]](#)
6. Al-Saydeh, S.A.; El-Naas, M.H.; Zaidi, S.J. Copper Removal from Industrial Wastewater: A Comprehensive Review. *J. Ind. Eng. Chem.* **2017**, *56*, 35–44. [\[CrossRef\]](#)

7. Ab Hamid, N.H.; bin Mohd Tahir, M.I.H.; Chowdhury, A.; Nordin, A.H.; Alshaikh, A.A.; Suid, M.A.; Nazaruddin, N.H.; Nozaizeli, N.D.; Sharma, S.; Rushdan, A.I. The Current State-Of-Art of Copper Removal from Wastewater: A Review. *Water* **2022**, *14*, 3086. [[CrossRef](#)]
8. Karim, N. Copper and Human Health—A Review. *J. Bahria Univ. Med. Dent. Coll.* **2018**, *08*, 117–122. [[CrossRef](#)]
9. Krstić, V.; Urošević, T.; Pešovski, B. A Review on Adsorbents for Treatment of Water and Wastewaters Containing Copper Ions. *Chem. Eng. Sci.* **2018**, *192*, 273–287. [[CrossRef](#)]
10. Pontius, F.W. Defining a Safe Level for Copper in Drinking Water. *J. Am. Water Works Assoc.* **1998**, *90*, 18–102. [[CrossRef](#)]
11. Gorchev, H.G.; Ozolins, G. WHO Guidelines for Drinking-Water Quality. *WHO Chron.* **1984**, *38*, 104–108. [[PubMed](#)]
12. Demirkiran, N.; Künkül, A. Recovering of Copper with Metallic Aluminum. *Trans. Nonferr. Met. Soc. China* **2011**, *21*, 2778–2782. [[CrossRef](#)]
13. Elimelech, M.; Phillip, W.A. The Future of Seawater Desalination: Energy, Technology, and the Environment. *Science* **2011**, *333*, 712–717. [[CrossRef](#)]
14. Algieri, C.; Chakraborty, S.; Candamano, S. A Way to Membrane-Based Environmental Remediation for Heavy Metal Removal. *Environments* **2021**, *8*, 52. [[CrossRef](#)]
15. Lucaci, A.R.; Bulgariu, D.; Popescu, M.-C.; Bulgariu, L. Adsorption of Cu(II) Ions on Adsorbent Materials Obtained from Marine Red Algae *Callithamnion corymbosum* sp. *Water* **2020**, *12*, 372. [[CrossRef](#)]
16. Shi, J.; Yang, Z.; Dai, H.; Lu, X.; Peng, L.; Tan, X.; Shi, L.; Fahim, R. Preparation and Application of Modified Zeolites as Adsorbents in Wastewater Treatment. *Water Sci. Technol.* **2018**, *2017*, 621–635. [[CrossRef](#)]
17. González Vázquez, O.F.; del Moreno Virgen, M.R.; Hernández Montoya, V.; Tovar Gómez, R.; Alcántara Flores, J.L.; Pérez Cruz, M.A.; Montes Morán, M.A. Adsorption of Heavy Metals in the Presence of a Magnetic Field on Adsorbents with Different Magnetic Properties. *Ind. Eng. Chem. Res.* **2016**, *55*, 9323–9331. [[CrossRef](#)]
18. Skoczko, I.; Szatyłowicz, E. Removal of Heavy Metal Ions by Filtration on Activated Alumina-Assisted Magnetic Field. *Desalin. Water Treat.* **2018**, *117*, 345–352. [[CrossRef](#)]
19. Szatyłowicz, E.; Skoczko, I. Magnetic Field Usage Supported Filtration Through Different Filter Materials. *Water* **2019**, *11*, 1584. [[CrossRef](#)]
20. Szatyłowicz, E.; Skoczko, I. The Use of Activated Alumina and Magnetic Field for the Removal Heavy Metals from Water. *J. Ecol. Eng.* **2018**, *19*, 61–67. [[CrossRef](#)]
21. Zafar, S.; Khan, M.I.; Lashari, M.H.; Khraisheh, M.; Almomani, F.; Mirza, M.L.; Khalid, N. Removal of Copper Ions from Aqueous Solution Using NaOH-Treated Rice Husk. *Emergent Mater.* **2020**, *3*, 857–870. [[CrossRef](#)]
22. Wang, Z.; Huang, G.; An, C.; Chen, L.; Liu, J. Removal of Copper, Zinc and Cadmium Ions through Adsorption on Water-Quenched Blast Furnace Slag. *Desalin. Water Treat.* **2016**, *57*, 22493–22506. [[CrossRef](#)]
23. Yehia, A.; El-Rahiem, A.F.H.; El-Taweel, R.S. Removal of Heavy Metals from Aqueous Solutions by Unburned Carbon Separated from Blast Furnace Flue Dust. *Miner. Process. Extr. Metall.* **2008**, *117*, 205–208. [[CrossRef](#)]
24. Buema, G.; Harja, M.; Lupu, N.; Chiriac, H.; Forminte, L.; Ciobanu, G.; Bucur, D.; Bucur, R. Adsorption Performance of Modified Fly Ash for Copper Ion Removal from Aqueous Solution. *Water* **2021**, *13*, 207. [[CrossRef](#)]
25. Harja, M.; Buema, G.; Sutiman, D.-M.; Munteanu, C.; Bucur, D. Low Cost Adsorbents Obtained from Ash for Copper Removal. *Korean J. Chem. Eng.* **2012**, *29*, 1735–1744. [[CrossRef](#)]
26. Liu, H.; Mo, Z.; Li, L.; Chen, F.; Wu, Q.; Qi, L. Efficient Removal of Copper(II) and Malachite Green from Aqueous Solution by Magnetic Magnesium Silicate Composite. *J. Chem. Eng. Data* **2017**, *62*, 3036–3042. [[CrossRef](#)]
27. Huang, R.; Wu, M.; Zhang, T.; Li, D.; Tang, P.; Feng, Y. Template-Free Synthesis of Large-Pore-Size Porous Magnesium Silicate Hierarchical Nanostructures for High-Efficiency Removal of Heavy Metal Ions. *ACS Sustain. Chem. Eng.* **2017**, *5*, 2774–2780. [[CrossRef](#)]
28. Liu, K.; Zhu, B.; Feng, Q.; Wang, Q.; Duan, T.; Ou, L.; Zhang, G.; Lu, Y. Adsorption of Cu(II) Ions from Aqueous Solutions on Modified Chrysotile: Thermodynamic and Kinetic Studies. *Appl. Clay Sci.* **2013**, *80–81*, 38–45. [[CrossRef](#)]
29. Choong, C.; Lee, G.; Jang, M.; Park, C.; Ibrahim, S. One Step Hydrothermal Synthesis of Magnesium Silicate Impregnated Palm Shell Waste Activated Carbon for Copper Ion Removal. *Metals* **2018**, *8*, 741. [[CrossRef](#)]
30. Acharya, P.K.; Patro, S.K. Utilization of Ferrochrome Wastes Such as Ferrochrome Ash and Ferrochrome Slag in Concrete Manufacturing. *Waste Manag. Res. J. Sustain. Circ. Econ.* **2016**, *34*, 764–774. [[CrossRef](#)]
31. Krishna, R.S.; Mishra, J.; Zribi, M.; Adeniyi, F.; Saha, S.; Baklouti, S.; Shaikh, F.U.A.; Gökçe, H.S. A Review on Developments of Environmentally Friendly Geopolymer Technology. *Materialia* **2021**, *20*, 101212. [[CrossRef](#)]
32. Omur, T.; Miyan, N.; Kabay, N.; Birol, B.; Oktay, D. Characterization of Ferrochrome Ash and Blast Furnace Slag Based Alkali-Activated Paste and Mortar. *Constr. Build. Mater.* **2023**, *363*, 129805. [[CrossRef](#)]
33. Du Preez, S.P.; Beukes, J.P.; Van Dalen, W.P.J.; Van Zyl, P.G.; Paktunc, D.; Looock-Hattingh, M.M. Aqueous Solubility of Cr(VI) Compounds in Ferrochrome Bag Filter Dust and the Implications Thereof. *Water SA* **2017**, *43*, 298. [[CrossRef](#)]
34. Lin, L.C.; Thirumavalavan, M.; Wang, Y.T.; Lee, J.F. Surface Area and Pore Size Tailoring of Mesoporous Silica Materials by Different Hydrothermal Treatments and Adsorption of Heavy Metal Ions. *Colloids Surf. A Physicochem. Eng. Asp.* **2010**, *369*, 223–231. [[CrossRef](#)]
35. Prasad, M.; Saxena, S. Sorption Mechanism of Some Divalent Metal Ions Onto Low-Cost Mineral Adsorbent. *Ind. Eng. Chem. Res.* **2004**, *43*, 1512–1522. [[CrossRef](#)]

36. Wang, X.; Qin, Y. Equilibrium Sorption Isotherms for of Cu^{2+} on Rice Bran. *Process Biochem.* **2005**, *40*, 677–680. [[CrossRef](#)]
37. Aksu, Z.; İsoğlu, İ.A. Removal of Copper(II) Ions from Aqueous Solution by Biosorption onto Agricultural Waste Sugar Beet Pulp. *Process Biochem.* **2005**, *40*, 3031–3044. [[CrossRef](#)]
38. Rafatullah, M.; Sulaiman, O.; Hashim, R.; Ahmad, A. Adsorption of Copper (II) onto Different Adsorbents. *J. Dispers. Sci. Technol.* **2010**, *31*, 918–930. [[CrossRef](#)]
39. Zenasni, M.A.; Benfarhi, S.; Merlin, A.; Molina, S.; George, B.; Meroufel, B. Adsorption of Cu(II) on Maghnite from Aqueous Solution: Effects of PH, Initial Concentration, Interaction Time and Temperature. *Nat. Sci.* **2012**, *4*, 856–868. [[CrossRef](#)]
40. Kleiv, R.; Sandvik, K. Modelling Copper Adsorption on Olivine Process Dust Using a Simple Linear Multivariable Regression Model. *Miner. Eng.* **2002**, *15*, 737–744. [[CrossRef](#)]
41. Darmayanti, L.; Notodarmodjo, S.; Damanhuri, E. Removal of Copper (II) Ions in Aqueous Solutions by Sorption onto Fly Ash. *J. Eng. Technol. Sci.* **2017**, *49*, 546–559. [[CrossRef](#)]
42. Abbar, B.; Alem, A.; Marcotte, S.; Pantet, A.; Ahfir, N.D.; Bizet, L.; Duriatti, D. Experimental Investigation on Removal of Heavy Metals (Cu^{2+} , Pb^{2+} , and Zn^{2+}) from Aqueous Solution by Flax Fibres. *Process Saf. Environ. Prot.* **2017**, *109*, 639–647. [[CrossRef](#)]
43. Jellali, S.; Azzaz, A.; Jeguirim, M.; Hamdi, H.; Mlayah, A. Use of Lignite as a Low-Cost Material for Cadmium and Copper Removal from Aqueous Solutions: Assessment of Adsorption Characteristics and Exploration of Involved Mechanisms. *Water* **2021**, *13*, 164. [[CrossRef](#)]
44. Huang, P.; Li, Z.; Chen, M.; Hu, H.; Lei, Z.; Zhang, Q.; Yuan, W. Mechanochemical Activation of Serpentine for Recovering Cu (II) from Wastewater. *Appl. Clay Sci.* **2017**, *149*, 1–7. [[CrossRef](#)]
45. Petrounias, P.; Rogkala, A.; Giannakopoulou, P.P.; Lampropoulou, P.; Koutsovitis, P.; Koukouzas, N.; Laskaris, N.; Pomonis, P.; Hatzipanagiotou, K. Removal of Cu (II) from Industrial Wastewater Using Mechanically Activated Serpentinite. *Energies* **2020**, *13*, 2228. [[CrossRef](#)]
46. Chowdhury, Z.Z.; Sharifuddin, M.Z.; Khan, R.A.; Khalid, K. Linear Regression Analysis for Kinetics and Isotherm Studies of Sorption of Manganese (II) Ions onto Activated Palm Ash from Waste Water. *Orient. J. Chem.* **2011**, *27*, 405–415.
47. Darmayanti, L.; Notodarmojo, S.; Damanhuri, E.; Kadja, G.T.M.; Mukti, R.R. Preparation of Alkali-Activated Fly Ash-Based Geopolymer and Their Application in the Adsorption of Copper (II) and Zinc (II) Ions. In Proceedings of the International Conference on Advances in Civil and Environmental Engineering (ICAnCEE 2018), Bali, Indonesia, 24–25 October 2018; Olivia, M., Marto, A., Yamamoto, K., Wishart, D., Saputra, E., Ketut Sudarsana, I.D., Agus Ariawan, I.M., Infantri Yekti, M., Ridwan, R., Wibisono, G., et al., Eds.; MATEC Web of Conferences. EDP Science: Les Ulis, France, 2019; Volume 276, p. 06012.
48. Abdalqader, A.F.; Jin, F.; Al-Tabbaa, A. Development of Greener Alkali-Activated Cement: Utilisation of Sodium Carbonate for Activating Slag and Fly Ash Mixtures. *J. Clean. Prod.* **2016**, *113*, 66–75. [[CrossRef](#)]
49. Qiu, J.; Zhao, Y.; Xing, J.; Sun, X. Fly Ash/Blast Furnace Slag-Based Geopolymer as a Potential Binder for Mine Backfilling: Effect of Binder Type and Activator Concentration. *Adv. Mater. Sci. Eng.* **2019**, *2019*, 2028109. [[CrossRef](#)]
50. Choudhary, R.; Koppala, S.; Swamiappan, S. Bioactivity Studies of Calcium Magnesium Silicate Prepared from Eggshell Waste by Sol–Gel Combustion Synthesis. *J. Asian Ceram. Soc.* **2015**, *3*, 173–177. [[CrossRef](#)]
51. Fu, H.; Ding, X.; Ren, C.; Li, W.; Wu, H.; Yang, H. Preparation of Magnetic Porous $\text{NiFe}_2\text{O}_4/\text{SiO}_2$ Composite Xerogels for Potential Application in Adsorption of Ce(IV) Ions from Aqueous Solution. *RSC Adv.* **2017**, *7*, 16513–16523. [[CrossRef](#)]
52. Poorsargol, M.; Razmara, Z.; Amiri, M.M. The Role of Hydroxyl and Carboxyl Functional Groups in Adsorption of Copper by Carbon Nanotube and Hybrid Graphene–Carbon Nanotube: Insights from Molecular Dynamic Simulation. *Adsorption* **2020**, *26*, 397–405. [[CrossRef](#)]
53. Chen, J.P.; Wu, S. Simultaneous Adsorption of Copper Ions and Humic Acid onto an Activated Carbon. *J. Colloid Interface Sci.* **2004**, *280*, 334–342. [[CrossRef](#)] [[PubMed](#)]
54. Al-Qunaibit, M.H.; Mekhemer, W.K.; Zaghoul, A.A. The Adsorption of Cu(II) Ions on Bentonite—A Kinetic Study. *J. Colloid Interface Sci.* **2005**, *283*, 316–321. [[CrossRef](#)]
55. Li, J.; Hu, J.; Sheng, G.; Zhao, G.; Huang, Q. Effect of PH, Ionic Strength, Foreign Ions and Temperature on the Adsorption of Cu(II) from Aqueous Solution to GMZ Bentonite. *Colloids Surf. A Physicochem. Eng. Asp.* **2009**, *349*, 195–201. [[CrossRef](#)]
56. Glatstein, D.A.; Francisca, F.M. Influence of PH and Ionic Strength on Cd, Cu and Pb Removal from Water by Adsorption in Na-Bentonite. *Appl. Clay Sci.* **2015**, *118*, 61–67. [[CrossRef](#)]
57. Ho, Y.S.; McKay, G. Sorption of Dyes and Copper Ions onto Biosorbents. *Process Biochem.* **2003**, *38*, 1047–1061. [[CrossRef](#)]
58. Onundi, Y.B.; Mamun, A.A.; Khatib, M.F.; Ahmed, Y.M. Adsorption of Copper, Nickel and Lead Ions from Synthetic Semiconductor Industrial Wastewater by Palm Shell Activated Carbon. *Int. J. Environ. Sci. Technol.* **2010**, *7*, 751–758. [[CrossRef](#)]

Disclaimer/Publisher’s Note: The statements, opinions and data contained in all publications are solely those of the individual author(s) and contributor(s) and not of MDPI and/or the editor(s). MDPI and/or the editor(s) disclaim responsibility for any injury to people or property resulting from any ideas, methods, instructions or products referred to in the content.